Molecular Pharmacology 107 (2025) 100031

Molecular Pharmacology

journal homepage: www.molpharm.aspetjournals.org

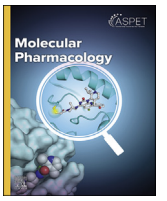

ARTICLE

Multiwalled carbon nanotubes activate the NLRP3 inflammasome-dependent pyroptosis in macrophages

Chol Seung Lim [1], Ja Kook Gu [2], Qiang Ma [1,*]

[1] Receptor Biology Laboratory, Toxicology and Molecular Biology Branch, Health Effects Laboratory Division, National Institute for Occupational Safety and Health, Centers for Disease Control and Prevention, Morgantown, West Virginia

[2] BioAnalytics Branch, Health Effects Laboratory Division, National Institute for Occupational Safety and Health, Centers for Disease Control and Prevention, Morgantown, West Virginia

ARTICLE INFO

Article history:
Received 3 January 2025
Accepted 13 March 2025
Available online 2 April 2025

Key words:
IL-1β
Inflammation
M1 macrophage
MWCNT
NLRP3
Pyroptosis

ABSTRACT

Macrophages are major innate immune cells for the clearance of inhaled nanoparticles but may undergo cell death upon phagocytosis of certain nanoparticles due to their resistance to lysosomal degradation and high toxicity to the cell. Here we investigated the pyroptotic effect of exposure to fibrogenic multiwalled carbon nanotubes (MWCNTs) on macrophages, an inflammatory form of cell death. We first evaluated MWCNT-induced cell death in M1 and M2 macrophages that mediate the temporal inflammatory response to MWCNTs in mammalian lungs. Macrophages were differentiated from human monocytic THP-1 cells, followed by polarization to M1 or M2 cells. MWCNTs caused concentration- and time-dependent cytotoxicity in M1 and, to a lesser extent, M2 cells. Carbon black, an amorphous carbonous material control for CNTs, did not cause apparent toxicity in the cells. MWCNTs increased the production and secretion of IL-1β, accompanied by activation of caspase-1, in M1, but not M2, cells. Moreover, MWCNTs induced the formation of apoptosis-associated speck-like protein containing a C-terminal caspase recruitment domain specks and the release of cathepsin B in M1 cells, revealing activation of the nucleotide-binding, oligomerization domain-like receptor family pyrin domain containing 3 (NLRP3) inflammasome via lysosomal damage. MWCNTs induced the cleavage of gasdermin D (GSDMD) to form the 31 kDa N-terminal fragment (GSDMD-N), the pore-forming peptide causing pyroptotic cell death. Increased IL-1β release was completely suppressed by AC-YVAD-CMK (a caspase-1 inhibitor), MCC-950 (an NLRP3 inflammasome inhibitor), or CA-074 Me (a cathepsin B inhibitor), alongside the blockage of MWCNT-induced cleavage of GSDMD. The study demonstrates that MWCNTs trigger pyroptosis in M1 macrophages and boost sterile inflammation by activating the NLRP3 inflammasome pathway.

Significance Statement: The nucleotide-binding, oligomerization domain-like receptor family pyrin domain containing 3 inflammasome mediates the inflammatory response to fibrogenic nanoparticles in the lung via multiple means. The current study uncovers the induction of pyroptotic death of macrophages as a major means of nanotoxicity and sterile inflammation via the nucleotide-binding, oligomerization domain-like receptor family pyrin domain containing 3 pathway by nanoparticles.

Published by Elsevier Inc. on behalf of American Society for Pharmacology and Experimental Therapeutics.

1. Introduction

Pulmonary exposure to fibrogenic carbon nanotubes (CNTs) causes inflammation that can progress to fibrosis and malignancy in mammalian lungs (Donaldson et al, 2006; Dong and Ma, 2015). Macrophages are major innate immune cells to defend against infection and injury by multiple means (Wynn et al, 2013). In the lung, macrophages differentiate into polarized cells to instigate

* **Address correspondence to:** Dr Qiang Ma, Receptor Biology Laboratory, Toxicology and Molecular Biology Branch, Health Effects Laboratory Division, National Institute for Occupational Safety and Health, Centers for Disease Control and Prevention, 1000 Frederick Lane, Morgantown, WV 26508. E-mail: qam1@cdc.gov

https://doi.org/10.1016/j.molpha.2025.100031
0026-895X/Published by Elsevier Inc. on behalf of American Society for Pharmacology and Experimental Therapeutics.

pulmonary inflammation to promote the clearance of inhaled pathogens and sterile insults, as well as the debridement and repair of lung tissue, in an inducer- and context-dependent manner (Wynn and Vannella, 2016; Lim et al, 2020; Ma, 2020). Fibrogenic CNTs are resistant to lysosomal breakdown and cause the death of phagocytes that engulf the CNTs, leading to characteristic sterile inflammation and, ultimately, persistent adverse outcomes, such as fibrosis and malignancy, in the lung and pleura (Dong and Ma, 2019).

Polarization enables macrophages to adopt distinct phenotypes and functions with certain plasticity (Murray et al, 2014). M1 macrophages (classically activated macrophages) exhibit T-helper (Th) 1-associated functions including promotion of acute inflammation, destruction of the extracellular matrix (ECM), and cell death (Wynn and Barron, 2010). Exposure to interferon (IFN)-γ, followed by lipopolysaccharides (LPS), is commonly used to induce M1 polarization. M2 macrophages (alternatively activated macrophages) have Th2-associated phenotypes important for tissue repair, angiogenesis, resolution of inflammation, and fibrosis. Differentiation into M2 macrophages requires the presence of IL-4 and/or IL-13. Upon exposure to certain multiwalled CNTs (MWCNTs), such as the rod-like Mitsui-7 MWCNTs, macrophages in the lung polarize to M1 cells to mediate the initiation and amplification of acute inflammation. M2 polarization occurs subsequently and promotes the resolution of inflammation and repair of lung damage (Dong and Ma, 2016; 2018a,b; Lim et al, 2020, 2023).

Polarized M1 and M2 cells regulate inflammation locally and systemically by producing proinflammatory and proresolving molecules in mice exposed to respirable particles (Ma, 2020). The proinflammatory cytokine IL-1β is a major cytokine secreted by activated monocytes and macrophages upon stimulation by MWCNTs. IL-1β has pleotropic effects including neutrophil recruitment, pyrogenic effect, and promotion of cell proliferation and cell death. Induction and maturation of IL-1β is dependent on the activation of the NOD-like receptor family pyrin domain containing 3 (NLRP3) inflammasome, a cytoplasmic multiprotein complex formed in response to diverse stimuli to orchestrate innate immune responses (Schroder and Tschopp, 2010; Ma and Lim, 2024).

Formation of the NLRP3 inflammasome involves a set of defined molecular events (Tschopp and Schroder, 2010). Quiescent NLRP3 is activated by specific signals called pathogen-associated molecular patterns and damage/danger-associated molecular patterns. Activated NLRP3 associates with the apoptosis-associated speck-like protein containing a C-terminal caspase recruitment domain (ASC). The NLRP3-ASC complex oligomerizes and recruits procaspase-1, forming an active inflammasome (Ma, 2023). Recruited procaspase-1 is activated via proximity autoactivation to become caspase-1. Caspase-1 cleaves pro-IL-1β to form active IL-1β, which is subsequently secreted into the extracellular matrix and the circulation. Known activators of NLRP3 include ATP, nigericin, microbial pathogens, such as *Listeria monocytogenes* and *Streptococcus pneumonia*, and sterile particulate stimuli, such as silica and aluminum hydroxide. At the molecular level, potassium efflux, release of lysosomal cathepsin B, and generation of reactive oxygen species (ROS) constitute the initial steps to activate the NLRP3 inflammasome by both microbial and sterile signals. Variations in the sensing and effector mechanisms of different stimuli are noted but not well understood (Chen and Nuñez, 2010; Swanson et al, 2019; Ma, 2023).

Pyroptosis is a form of inflammatory cell death that is triggered by proinflammatory signals and heightens inflammation by releasing the engulfed pathogens and particles, inflammatory mediators, and cell debris from pyroptotic cells (Cookson and Brennan, 2001; Broz et al, 2020). Pyroptotic cell death is caspase-1-dependent (Liu et al, 2016). The proteolytic cleavage of gasdermin D (GSDMD) by caspase-1 allows for the insertion of its N-terminal fragment (GSDMD-N) into the plasma membrane, leading to pore formation and pyroptotic cell death (Shi et al, 2015). Exposure to MWCNTs, such as Mitsui-7, at certain doses, causes cell death in the lung and in vitro (He et al, 2011; Palomäki et al, 2011; Hindman and Ma, 2019; Keshavan et al, 2021). MWCNTs have been shown to induce the secretion of IL-1β and activation of the NLRP3 inflammasome in mouse lungs and cultured cells (Dong et al, 2015; Jessop and Holian, 2015; Hindman and Ma, 2019; Porter et al, 2020). The mechanism by which the MWCNTs induce cell death of macrophages in relation to polarization and inflammation remains to be elucidated.

Given the pivotal role of macrophages and pyroptosis in inflammation, we investigated the pyroptotic effect of MWCNTs on macrophages. Specifically, we characterized the differential cytotoxicity of MWCNTs to M1 and M2 cells. The findings demonstrate activation of the NLRP3 inflammasome pathway by MWCNTs in M1, but not M2, macrophages to result in the production and maturation of IL-1β and pyroptotic death of M1 cells. This study provides new insights into the mechanism by which MWCNTs cause the pyroptotic death of macrophages by activating the NLRP3 inflammasome pathway, which boosts sterile inflammation and may lead to progressive and chronic outcomes.

2. Materials and methods

2.1. Particle preparation

MWCNTs were obtained from Mitsui & Company (Mitsui-7, XNRI 1, lot #-05072001K28). Carbon black (CB) was purchased commercially (Printex 90, Degussa Engineered Carbons, L.P.). CB are amorphous, carbonaceous particulates and therefore are used as a nonfiber, carbon-based particle material control for MWCNTs. MWCNTs and CB were dispersed in Dulbecco's Modified Eagle Medium with 1% fetal bovine serum (FBS; both from Thermo Fisher Scientific) at a concentration of 2 mg/mL by vortex and sonication as described previously (Hindman and Ma, 2019; Lim et al, 2023). Properties of the MWCNTs and CB have been characterized and reported previously (Porter et al, 2010; Lim et al, 2020, 2023). The levels of LPS in the MWCNT and CB preparations were determined to be <0.1 EU/mL (<0.01 mg/mL) by using the Pierce LAL chromogenic endotoxin quantification kit (Thermo Scientific). For cell treatment, stock solutions were diluted with the culture media, and the dilution preparation for treatment was sonicated and vortexed immediately before use. The control medium (Dulbecco's modified Eagle's medium plus 1% FBS) was prepared and used to establish a baseline response. Some cells were kept untreated and used as a cell background control. All cells were treated in duplicates, and all treatments were conducted for 3 times.

2.2. Cell culture and treatment

The human acute monocytic cell line THP-1 was acquired from American Type Culture Collection and maintained in the Roswell Park Memorial Institute-1640 medium containing Glutamax and HEPES and supplemented with 1× antibiotic-antimycotic and 10% heat-inactivated FBS (Thermo Fisher Scientific). Cells were maintained at 37 °C in a humidified 5% CO_2 incubator. Cells were passaged at a cell density of up to 5.0×10^5 cells/mL every 3–4 days. Cells from passage 4–10 were used in this experiment.

To differentiate cells into adherent, macrophage-like cells, THP-1 cells were plated at a cell density of 5.0×10^5 cells/mL and incubated for 3 days in the presence of 40 nM phorbol-12-myristate-13-acetate

(Sigma-Aldrich). Polarization into M1 macrophages was induced by incubation of differentiated THP-1 cells with IFN-γ at 20 ng/mL plus LPS at 100 ng/mL (both from Sigma-Aldrich) for 2 days. Polarization into M2 cells was induced by incubation with IL-4 (Sigma-Aldrich) at 20 ng/mL for 2 days. Polarized M1 and M2 cells were washed with warm, sterile PBS and were exposed to MWCNTs or CB for 1 or 3 days at concentrations indicated in figures. Inhibition of the NLRP3 inflammasome pathway and pyroptosis was carried out by using the caspase-1 inhibitor AC-YVAD-CMK at 25 and 50 μg/mL, the NLRP3 inflammasome inhibitor MCC-950 at 0.5 and 1 μM, and the cathepsin B inhibitor CA-074 methyl ester (CA-074 Me) at 50 and 100 μM (All from Sigma-Aldrich) for 6 hours before the cells were exposed to MWCNTs or CB.

For experiments on the NLRP3 inflammasome, differentiated macrophages were primed with LPS at 100 ng/mL for 24 hours, followed by adenosine 5′-triphosphate (ATP) at 5 mM (both from Sigma-Aldrich) for an additional hour. As a positive control, nigericin at 10 μM (Cayman Chemicals) was applied to induce the NLRP3 inflammasome-mediated IL-1β release. After treatment, the culture medium was collected and centrifuged at 4 °C to remove particles, cells, and cell debris. The cell-free medium was used for the detection of cytokines by ELISA. After washing, the cells were collected and used for further analysis of cells and proteins.

2.3. Flow cytometry

Polarized M1 or M2 macrophages were incubated with an Fc block solution (1× PBS containing rat serum and 25 μg/mL unlabeled anti-CD16/CD32 antibody 2.4G2) for 5 minutes at room temperature. The cells were stained with the FITC-conjugated mouse anti-human CD86 [clone 2331 (FUN-1), #560958] or CD206 (clone 19.2, #551135) antibodies or its isotype-matched control mouse IgG antibody (all from BD Biosciences) for 25 minutes at 4 °C in the dark. The cells were washed with 1 mL of FACs buffer (1× PBS containing 2 mM EDTA and 5% FBS). The cells were fixed using the Cytofix buffer (BD Biosciences) for 10 minutes at room temperature, followed by washing with 1 mL of FACs buffer. Cells were resuspended in the FACs buffer, and flow cytometry was carried out on a BD LSR II flow cytometer (BD Biosciences). Data were analyzed using FlowJo software (V10.6).

2.4. ELISA

Cell culture media were collected from untreated cells (M0), or cells treated with IFN-γ+LPS for M1 cells or IL-4 for M2 cells. Cell-free culture supernatants were prepared by centrifugation at 800 × *g*, 4 °C to remove particles and cell debris. Inflammatory cytokines, that is, IL-1β, tumor necrosis factor-α (TNF-α), IL-10, and IL-13, were detected by ELISA.

For experiments on IL-1β release, M1 or M2 macrophages were untreated or treated with the control medium, MWCNTs at 2.5 μg or 10 μg/mL, CB at 2.5 μg or 10 μg/mL, or LPS followed by ATP (LPS+ATP), as described above under cell culture and treatment. For inhibition of the NLRP3 inflammasome pathway, cells were treated with AC-YVAD-CMK at 50 μg/mL, MCC-950 at 1 μM, or CA-074 Me at 100 μM for 6 hours before the treatment with MWCNTs at 2.5 or 10 μg/mL. IL-1β and TNF-α were detected by ELISA in cell-free culture supernatants. All ELISA kits were from MyBioSource, and measurement was performed by following the manufacturer's protocols.

2.5. Lactate dehydrogenase assay

Release of lactate dehydrogenase (LDH) from macrophages into the culture medium indicates cell damage/cell death and was determined using the CyQUANT LDH Cytotoxicity Assay (Thermo Fisher Scientific, C20300). Briefly, cells were seeded in 96-well plates at a density of 5×10^4 cells/well in the Roswell Park Memorial Institute-1640 medium. Following treatment, the cells were incubated with the LDH reaction mixture. Absorbance at 490 and 680 nm was measured, and LDH release was quantified using a BioTek synergy H1 multimode microplate reader (Agilent Technologies). As a control for interference from the absorption of light by particles, MWCNTs or CB were kept in the cell-free medium during LDH measurement. For calculation of the LDH activity, the 680 nm absorbance value (background) was subtracted from the 490 nm absorbance, and then, the % of cytotoxicity was calculated following the manufacturer's instructions. The experiments were repeated at least 3 times with duplicate measures performed at each treatment concentration.

2.6. Caspase-1 activity

M1 cells were untreated or treated with MWCNTs at 2.5 or 10 μg/mL, CB at 10 μg/mL, LPS at 100 ng/mL, or nigericin at 10 μM for 24 hours. For experiments on the NLRP3 inflammasome, cells were treated with MWCNTs at 10 μg/mL or LPS at 100 ng/mL for 24 hours, followed by 1 hour of incubation with 5 mM ATP. Cells were collected, centrifuged, and lysed for immediate use. Caspase-1 activity was measured using a colorimetric Caspase-1 activity assay kit (R&D Systems). Samples containing no cell lysate, or a substrate were included as negative controls.

2.7. Immunoblot

Macrophages were treated as indicated and were lysed in a lysis buffer (10 mM Tris, pH 7.4, 1% SDS) containing a proteinase inhibitor cocktail (Thermo Fisher Scientific). Cell lysates were collected and sonicated for 10 seconds. The supernatant was collected, and protein concentration was determined using a Bicinchoninic acid protein assay kit (Thermo Fisher Scientific). Lysate proteins of 10–20 μg each were resolved on a 10% SDS-PAGE gel and were transferred onto a nitrocellulose membrane. The membrane was incubated with 5% nonfat dry milk in Tris-buffered saline containing 0.05% Tween 20 for 1 hour at room temperature to block nonspecific binding before the incubation with primary antibodies. The primary antibodies used include rabbit anti-GSDMD (1:1000, Abcam, ab219800) for the detection of the full-length GSDMD, rabbit anti-GSDMD-N-term (1:1000, Abcam, ab215203) for detection of GSDMD-N, or mouse anti-β-actin (1:4000, Sigma-Aldrich, A5441) antibodies for loading control. After incubation with either the horseradish peroxidase-conjugated goat anti-mouse (1:5000, Jackson ImmunoResearch laboratories, 115-035-146) or the goat anti-rabbit IgG (1:5000, Jackson ImmunoResearch Laboratories, 111-035-144) antibody, immunoreactive bands were visualized using the Enhanced chemiluminescence substrates (Thermo Fisher Scientific). Band signals were captured onto X-ray film by exposure for 30 seconds, and the film was developed using a film processor (Konica Minolta). Scanned images were used to quantify band intensities using ImageJ software (NIH, USA), and each band was normalized to β-actin.

2.8. Immunofluorescence

The expression and localization of cleaved GSDMD, NLRP3, or ASC were examined using immunofluorescence staining and

fluorescent microscopy. THP-1 cells were seeded on chamber glass culture slides and differentiated and polarized into M1 cells as described above. The cells were untreated or treated with MWCNTs at 10 μg/mL, LPS plus ATP, or nigericin at 10 μM. The cells were fixed in 1% paraformaldehyde (w/v in 1× PBS), permeabilized in 0.5% Triton X-100 (v/v in 1X PBS), blocked in 5% normal goat serum (v/v in 1× PBS; all from Sigma-Aldrich), and stained with the rabbit anti-GSDMD-N-term (1:100, Abcam, ab215203), rabbit anti-NLRP3 (1:100, Thermo Fisher Scientific, PA520838), or mouse anti-ASC (1:50, Santa Cruz Biotechnology, sc-514414) antibodies in blocking buffer for overnight at 4 °C. Cells were then incubated with 1:1000 dilutions of Alexa 488 goat anti-rabbit or Alexa 555 goat anti-mouse IgG antibodies (Fisher Scientific) for 1 hour before being mounted in a photo-bleach resistant mounting medium containing the 4′,6-diamidino-2-phenylindole counterstain (Vector Labs). Cells were examined under a BX63 automated fluorescence microscope, and images were captured using a 63× oil objective. For colocalization of GSDMD-N-term and ASC, the same cells showing GSDND-N staining and ASC speck staining were counted using the ImageJ software. The percent of colocalization of GSDND-N and ASC was calculated from more than 100 cells for each treatment group. For ASC speck formation, cells showing ASC speck staining were counted and used for the calculation of percent positive cells from more than 100 cells for each treatment group.

2.9. Cathepsin B activity assay

Release of cathepsin B from lysosomes is a maker of lysosomal damage and was measured using the Magic Red fluorescent cathepsin B assay kit (Immunochemistry Technologies, 937). Briefly, cells were grown on a 96-well black-walled microplate (Fisher Scientific 07-000-135) at a cell density of 2.5×10^5 cells/mL and were treated as described above. After washing with 1× PBS (37 °C), the cells were stained with the Magic Red substrate reconstituted in DMSO. After incubation for 1 hour at 37 °C, fluorescence at excitation/emission of $\lambda = 592/628$ nm was measured using a Synergy H1 microplate reader (BioTek). The cathepsin B activity was calculated and expressed as fold changes for treated groups over controls.

2.10. Statistical analysis

Dependent measurements were analyzed using mixed-model 1-way analyses of variance, with each analysis incorporating the experiment as a random factor. For each experiment, the 2 replicate samples were averaged to give a single value for each treatment combination for each of the 3 independent experiments prepared on different days. For some variables, data were log-transformed to reduce heterogeneous variance and meet the assumptions of the analysis. Post-hoc comparisons were carried out using Fishers least significant difference test. All differences were considered significant at *, $P < .05$; **, $P < .01$; ***, $P < .001$; compared with untreated control or MWCNT-treated group. All analyses were carried out using the JMP version 16 software (SAS Institute).

3. Results

3.1. MWCNTs induced cytotoxicity in polarized macrophages

Polarized macrophages have distinct markers, metabolic and transcriptional profiles, and functions, which enable them to serve as major effector cells in inflammatory and immune responses under physiological and disease conditions (Wynn and Barron, 2010; Ma, 2020). Although fibrogenic MWCNTs have been shown to stimulate M1 and M2 polarization in animal lungs, few studies examined the effect of MWCNTs on polarized macrophages and their fate. Here, we took an in vitro approach to examine the interplay between inflammation and cell death of polarized macrophages upon exposure to MWCNTs.

Macrophages were differentiated from the human monocytic THP-1 cells with phorbol-12-myristate-13-acetate, followed by polarization to M1 or M2 cells with an M1 inducer LPS+ATP or M2 inducer IL-4, respectively. Polarized macrophages exhibited phenotypes of M1 or M2 cells as revealed by their cell surface markers and production of cytokines (Fig. 1). Expression of CD86 was evident after 2 days in M1, but not M2, macrophages, whereas expression of CD206 was markedly increased in M2, but not M1, macrophages (Fig. 1A). Production and secretion of type 1 and type 2 cytokines by polarized macrophages was examined after polarization was induced for 2 days. Cell-free media were assayed for production of IL-1β, TNF-α, IL-10, and IL-13 by ELISA. IL-1β was produced at 78.42 pg/mL by M1 macrophages, but only 18.37 pg/mL from M2 cells. Similar to IL-1β, TNF-α was detected at 27.71 pg/mL from M1 cells and only 2.37 pg/mL from M2 cells (Fig. 1B). On the contrary, IL-10 was at a high level (106.84 pg/mL) from M2 cells, but only at a low level (27.92 pg/mL) from M1 cells. IL-13 also showed 5.23-fold higher production and secretion from M2 than M1 cells (ie, 16.80 pg/mL from M2 versus 3.21 pg/mL from M1 cells; Fig. 1B).

We then evaluated the cellular damage to M1 and M2 cells from MWCNTs by measuring LDH release (Fig. 1C). The cells were exposed to increasing concentrations of MWCNTs as indicated for 1 or 3 days. MWCNTs triggered dose-dependent cell damage/cell death, which were significant at 50 μg/mL and 100 μg/mL of MWCNTs in M1 and, to a lesser extent, M2, macrophages (Fig. 1C). As a comparison, the amorphous carbon material control CB did not cause apparent cell damage in M1 and M2 macrophages, except there was a slight trend for CB to cause an increase in LDH release when tested at 100 μg/mL for 3 days in M1 macrophages (Fig. 1C). The results indicate that MWCNTs, but not CB, caused cell damage and cell death in both M1 and M2 cells, and M1 macrophages are more sensitive to the cytotoxic effect of MWCNTs than M2 cells.

3.2. MWCNTs activated the NLRP3 inflammasome to produce IL-1β in M1 cells

Given the prominent inflammatory effect of MWCNTs in the early phase of the pulmonary response, we examined the inflammatory status of the polarized cells in the presence of MWCNTs. We first compared the secretion of proinflammatory IL-1β from M1 and M2 macrophages exposed to MWCNTs or CB (Fig. 2). MWCNTs at 2.5 or 10 μg/mL induced IL-1β secretion from M1 macrophages with an increase of 2.3-fold or 3.9-fold, respectively, compared with either the untreated control or the control medium-treated cells. MWCNTs at 10 μg/mL slightly increased IL-1β secretion from M2 macrophages, which was not statistically significant. CB did not increase IL-1β secretion from either M1 or M2 macrophages. The NLRP3 inflammasome activator LPS plus ATP was used as a positive control. As expected, LPS plus ATP induced a high level of IL-1β from M1, but not M2, cells.

Production of IL-1β by macrophages requires the activation of caspase-1, which was examined in Fig. 2B. LPS at 100 ng/mL plus ATP at 5 mM (LPS+ATP) or nigericin at 10 μM was used as positive control, which caused large increases in the caspase-1 activity (31.83-fold for LPS+ATP and 36.22-fold for nigericin over control) in M1 cells, but much smaller increases (5.49-fold for LPS+ATP and 9.34-fold for nigericin) in M2 cells (Fig. 2B). LPS alone increased the caspase-1 activity in M1 macrophages by 17.02-fold. Treatment with MWCNTs at 2.5 or 10 μg/mL induced the caspase-1 activity by 7.33-fold and 14.96-fold over control, respectively. Interestingly, ATP was found to augment the increase in caspase-1 activity by

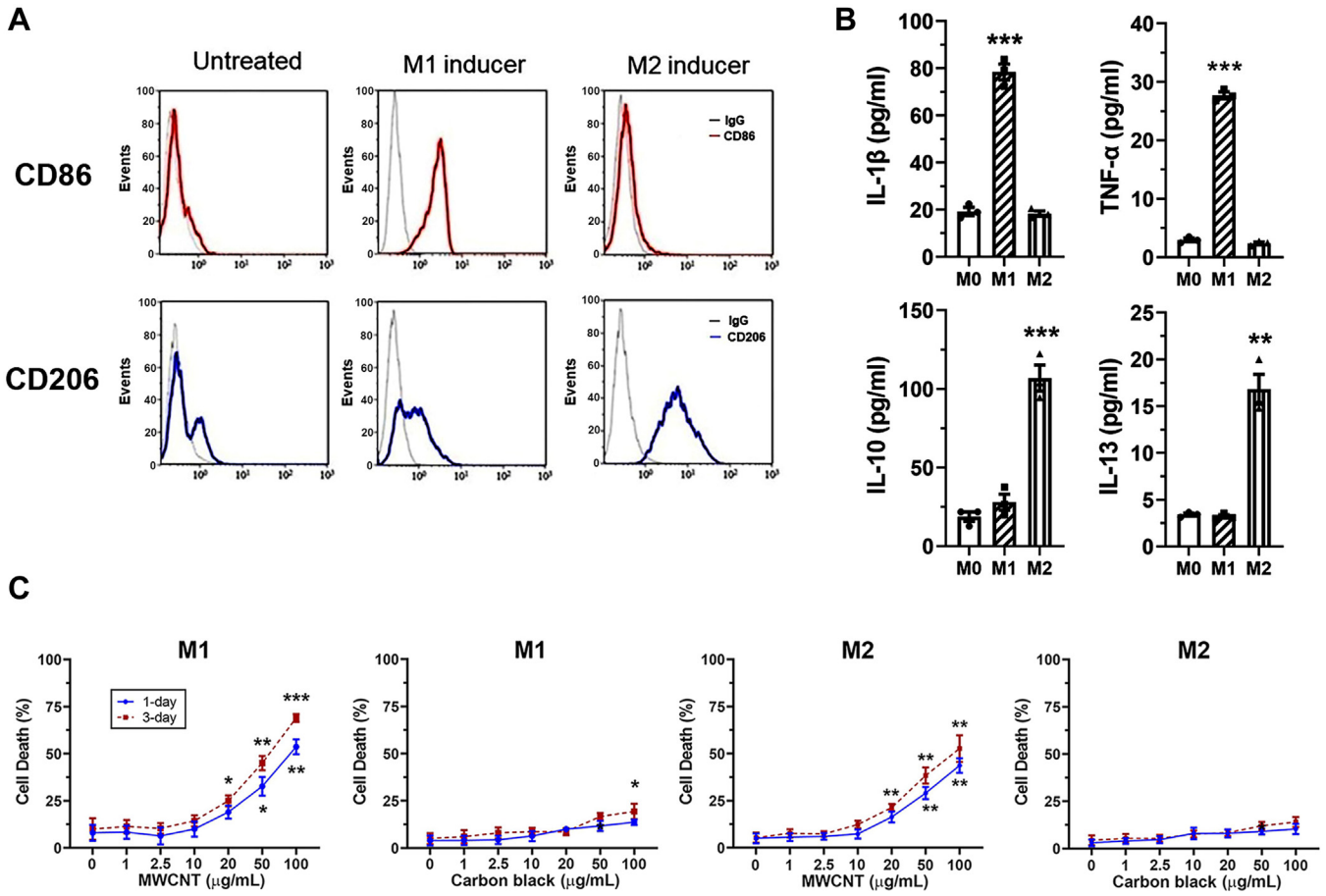

Fig. 1. Differential cytotoxicity of MWCNTs in polarized macrophages. (A) The human monocytic THP-1 cells were differentiated by 40 nM phorbol-12-myristate-13-acetate for 3 days. Cells were then polarized with either the M1 inducer IFN-γ at 20 ng/mL plus LPS at 100 ng/mL to obtain M1 macrophages or with the M2 inducer IL-4 at 20 ng/mL to obtain M2 macrophages. After 2 days of polarization, the cells were analyzed for expression of CD86 (M1 marker) or CD206 (M2 marker) on the cell surface by flow cytometry. The mouse IgG was used as a negative control. Representative histograms with each from 3 separate experiments were shown. (B) Inflammatory cytokines IL-1β, TNF-α, IL-10, and IL-13 in cell-free culture supernatants from M0 (unpolarized macrophages), M1, or M2 polarized macrophages were quantified by ELISA to serve as markers for M1 or M2 macrophages. Results represent mean ± SEM from 3 independent experiments. **, $P < .01$, and ***, $P < .001$, significance for comparison to "M0." (C) Cell viability was evaluated in M1 or M2 macrophages using the LDH assay after exposure to MWCNTs at 0, 1.0, 2.5, 10, 20, 50, or 100 μg/mL, or CB at 0, 1.0, 2.5, 10, 25, 50, 100 μg/mL for 1 day or 3 days. Data represent mean ± SEM (n = 3). *, $P < .05$, **, $P < .01$, and ***, $P < .001$, significance for comparison to "untreated control."

MWCNTs at 10 mg/mL, that is, a 25.48-fold increase by MWCNTs plus ATP, compared with the 14.96-fold increase by MWCNTs alone. CB at 10 μg/mL did not increase caspase-1 activity. In M2 macrophages, caspase-1 activation by MWCNTs was much lower than that in M1 macrophages; MWCNTs at 10 μg/mL induced caspase-1 activation by 4.35-fold increase, compared with untreated control. ATP slightly further increased the activity. LPS alone did not significantly increase caspase-1 activity in M2 macrophages.

Activation of caspase-1 indicates the activation of the NLRP3 inflammasome, which may require the release of the lysosome enzyme cathepsin B upon phagocytosis of MWCNTs by M1 macrophages (Ma and Lim, 2024). To examine the lysosomal integrity and release of lysosomal cathepsin B into the cytoplasm in MWCNT-exposed cells, we tested cathepsin B activity using a cathepsin B-specific substrate (Fig. 3A). MWCNTs at 2.5 or 10 mg/mL increased the release of cathepsin B at 24 hours post-exposure by 2.26-fold and 5.47-fold, respectively. No cathepsin B release was noted in cells exposed to CB at 10 μg/mL. LPS and LPS+ATP, but not nigericin (10 mM), caused significant increases in cathepsin B release. These results support the role of the lysosomal release of cathepsin B for NLRP3 activation by MWCNTs.

Activated NLRP3 assembles with the ASC protein through homotypic binding and directs the prion-like, directional oligomerization of ASC into filamentous bundles leading to the formation of ASC specks in the cytoplasm. For this reason, formation of ASC specks is often considered a marker of NLRP3 inflammasome activation in cells, although the ASC speck does not always colocalize with the NLRP3 inflammasome inside a cell. M1 macrophages in the absence of MWCNTs showed a diffused staining of ASC. MWCNTs at 10 μg/mL caused the formation of intensely stained ASC specks with a perinuclear localization (Fig. 3B). As expected, both positive controls, LPS+ATP and nigericin, induced marked increases in the formation of ASC specks in M1 macrophages.

Taken together, these findings presented a path of NLRP3 inflammasomal activation in M1 macrophages by MWCNTs, starting with the phagocytosis of CNTs, followed by lysosomal damage and release of lysosomal cathepsin B, which triggers the assembly of the NLRP3 inflammasome and formation of ASC specks, caspase-1 activation, and the maturation and secretion of IL-1β from M1 macrophages.

3.3. Activation of the NLRP3 inflammasome by MWCNTs led to GSDMD cleavage and pyroptosis of M1 macrophages

One consequence of NLRP3 activation is the activation of pyroptosis through the cleavage of GSDMD and pore formation by

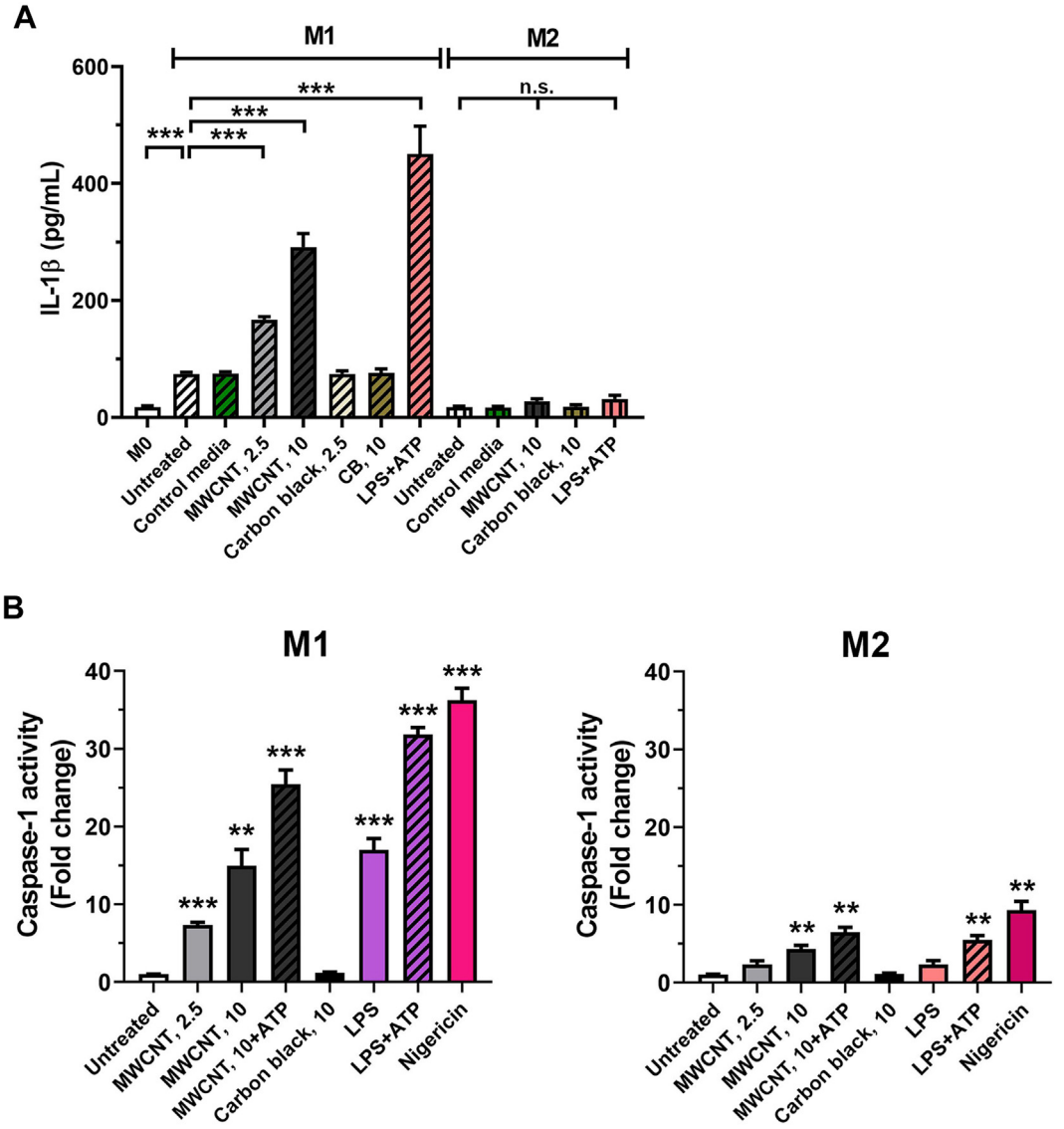

Fig. 2. Increased secretion of IL-1β and activation of caspase-1 in M1 macrophages by MWCNTs. (A) IL-1β secretion was assessed by ELISA in cell-free supernatants collected from differentiated THP-1 cells (M0), or polarized M1 or M2 macrophages that were untreated or exposed to the control medium, MWCNTs at 2.5 or 10 μg/mL, or CB at 2.5 or 10 μg/mL for 24 hours. Some cells were treated with LPS at 200 ng/mL for 24 hours followed by addition of ATP at 5 mM (ie, LPS+ATP) for 1 hour. Data represent mean ± SEM (n = 3). ***, $P <$ .001, significance for comparison to "M0" or "untreated"; n.s., non-significance at $P = .089$ for comparison between "MWCNT, 10" and "untreated," or $P = .103$ for comparison between "LPS+ATP" and "untreated" in M2 cells. (B) M1 or M2 macrophages were treated as described in (A) and were used to assess caspase-1 activity. Data represent mean ± SEM (n = 3). **, $P <$ .01, and ***, $P <$ .001, significance for comparison to "untreated" control.

the cleavage product, GSDMD-N, in the plasma membrane of the cell (Shi et al, 2015). Formation of the pores enables the secretion of mature IL-1β and IL-18 from the cell, as well as disruption of the osmotic gradient across the plasma membrane leading to the osmotic rupture, and pyroptotic death of the cell and release of the engulfed particles, inflammatory mediators, and other intracellular contents to amplify the inflammatory response. To examine GSDMD activation, M1 cells were treated with MWCNTs at 2.5 or 10 μg/mL, CB at 2.5 or 10 μg/mL, LPS at 100 ng/mL, LPS (100 ng/mL) + ATP (5 mM), or nigericin at 10 μM for 1 day. GSDMD and GSDMD-N were analyzed by immunoblotting using specific antibodies (Fig. 4A). MWCNTs at 2.5 or 10 μg/mL reduced the protein levels of GSDMD by 17.1% and 58.62%, respectively, compared with untreated control. LPS reduced the GSDMD level by approximately 21%. Addition of ATP to LPS further reduced the level by 18.15% (ie, 39.14% compared with untreated control). Nigericin strongly reduced the GSDMD level by 66.7%, compared with untreated control. CB did not affect the GSDMD protein level.

GSDMD-N was detected as a 31 kDa fragment. MWCNTs at 2.5 or 10 μg/mL increased the level of GSDMD-N by 423.5% or 557.3%, respectively, compared with untreated control. LPS increased the level by 398.2%, and the addition of ATP further increased the level by 170% (ie, 568.2%, compared with untreated control). Nigericin increased the level of GSDMD-M by 551.5%, compared with untreated control. CB slightly increased the N-terminal fragment level by 144.2% at 2.5 μg/mL and 134.9% at 10 μg/mL, compared with the untreated control, which was statistically not significant.

To validate if GSDMD cleavage and NLRP3 inflammasome activation are associated with each other in M1 macrophages, we examined the distribution of GSDMD-N in M1 cells using immunofluorescence imaging (Fig. 4B). Untreated cells exhibited no detectable GSDMD-N. MWCNTs at 10 μg/mL induced a diffuse

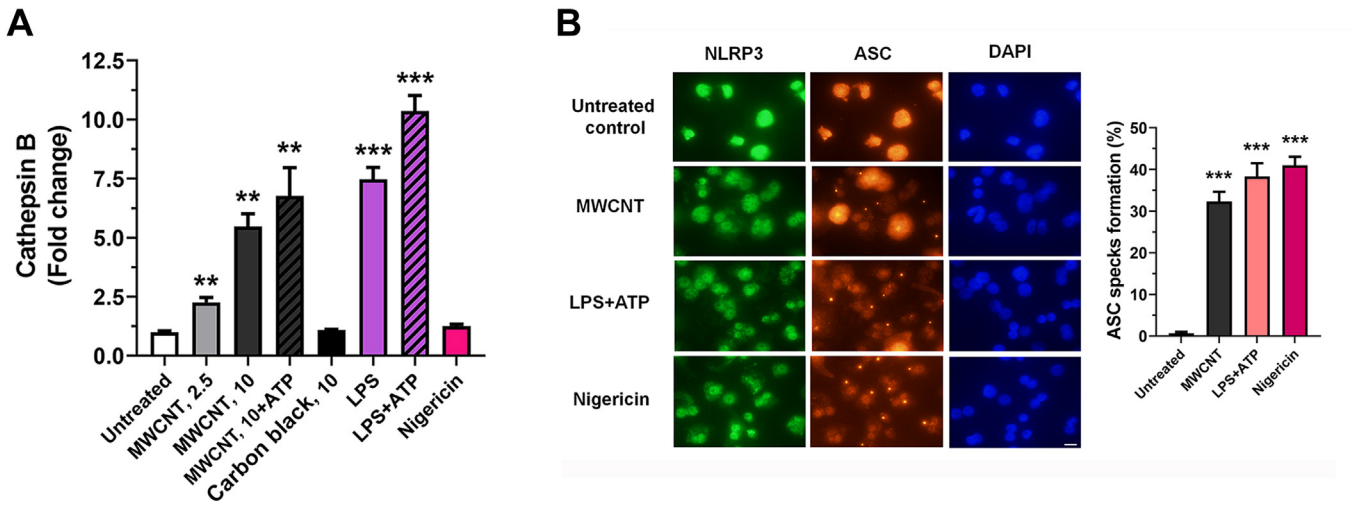

Fig. 3. Increased release of lysosomal cathepsin B and ASC speck formation in M1 macrophages by MWCNTs. (A) M1 macrophages were treated as described for Fig. 2 and were used to assess the cathepsin B activity using a fluorescent activity assay kit. Data represent mean ± SEM (n = 3). **, $P < .01$, ***, $P < .001$, significance for comparison to "untreated" control. (B) M1 macrophages were untreated or treated with MWCNTs at 10 μg/mL or nigericin at 10 μM for 24 hours. Some cells were treated with LPS at 200 ng/mL for 24 hours followed by the addition of ATP at 5 mM for 1 hour (ie, LPS+ATP). The cells were fixed and examined for immunofluorescent staining against NLRP3 (green channel), ASC (red), or 4′,6-diamidino-2-phenylindole (DAPI) (nucleus, blue). Fluorescence images were obtained and the cells having concentrated ASC staining were counted and expressed as percent of ASC specks formation. Data represent mean ± SEM (n = 3). ***, $P < .001$, significance for comparison to "untreated" control. *Scale bar*, 20 μm.

staining pattern of GSDMD-N. Inflammasome activators, LPS+ATP or nigericin, also induced a diffuse expression of GSDMD-N in M1 cells. In both cases, GSDMD-N colocalized with the ASC specks in significant numbers of cells as shown by the quantification of cells with positive colocalization. These results indicate that MWCNTs induced pyroptosis of M1 macrophages via the cleavage of GSDMD through the NLRP3 inflammasome-activated caspase-1.

3.4. Inhibition of the NLRP3 inflammasome pathway blocked pyroptosis

To substantiate the activation of the NLRP3 pathway and its role in M1 cell pyroptosis, various inhibitors were employed. As shown in Fig. 5A, the MWCNT-induced release of IL-1β into the medium is nearly completely inhibited by preincubation of the cells with specific caspase-1 inhibitor AC-YVAD-CMK at 50 μg/mL and by NLRP3 inflammasome inhibitor MCC-950 at 1 μM. Cathepsin B inhibitor CA-074 Me at 100 μM also blocked IL-1β production and secretion. However, the secretion of TNF-α, another major proinflammatory cytokine secreted by M1 macrophages in response to MWCNTs, was only slightly decreased by the inhibitors (Fig. 5B), indicating that induction of TNF-α in M1 macrophages by MWCNTs does not require the NLRP3 inflammasome.

Specific inhibitors were used to inhibit MWCNT-induced GSDMD cleavage in M1 macrophages (Fig. 5C). Treatment with caspase-1 inhibitor AC-YVAD-CMK at 25 μg/mL prior to MWCNTs

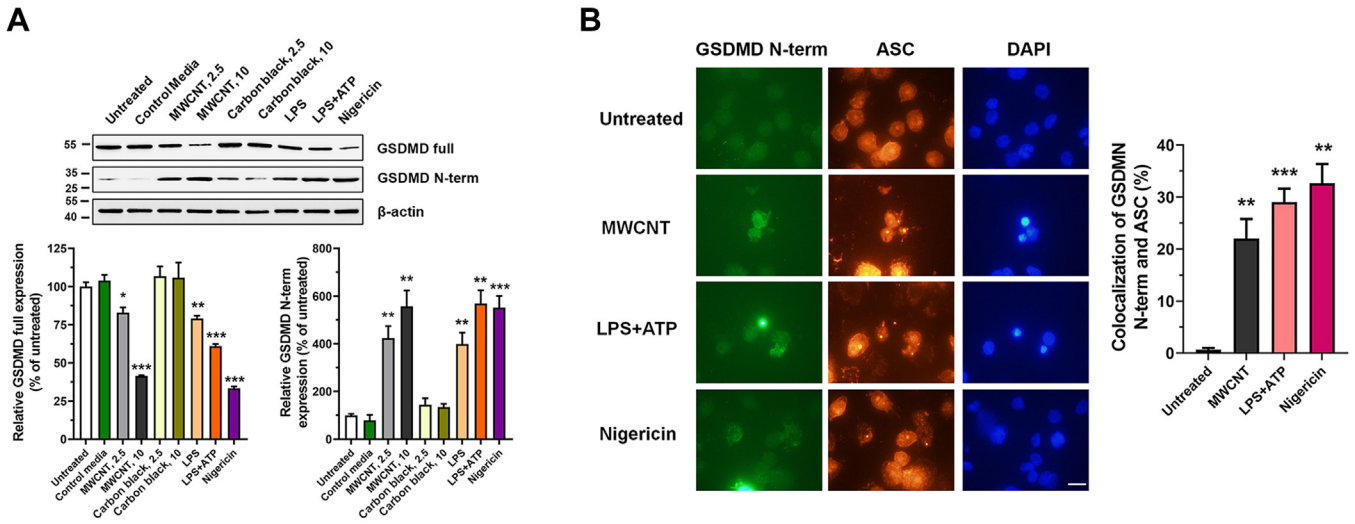

Fig. 4. Induced cleavage of in M1 macrophages by MWCNTs. M1 macrophages were untreated or treated with the control medium, MWCNTs at 2.5 or 10 μg/mL, CB at 2.5 or 10 μg/mL, LPS at 100 ng/mL, or nigericin at 10 μM for 24 hours. Some cells were treated with LPS at 200 ng/mL for 24 hours followed by the addition of ATP at 5 mM (ie, LPS+ATP) for 1 hour. (A) Cells were treated as shown and were harvested for immunoblotting of GSDMD and GSDMD-N. Representative images were shown with each from 3 experiments. Data represent mean ± SEM (n = 3). *, $P < .05$, **, $P < .01$, and ***, $P < .001$, significance for comparison to "untreated" control. (B) Cells treated as described in (A) were fixed and stained against GSDMD-N (green), ASC (red), or 4′,6-diamidino-2-phenylindole (DAPI) (blue) and were imaged using fluorescence microscopy. Cells showing both GSDMD-N and ASC staining were counted and expressed as the percentage of colocalization. Data represent mean ± SEM (n = 3). **, $P < .01$ and ***, $P < .001$, significance for comparison to untreated control. *Scale bar*, 20 μm.

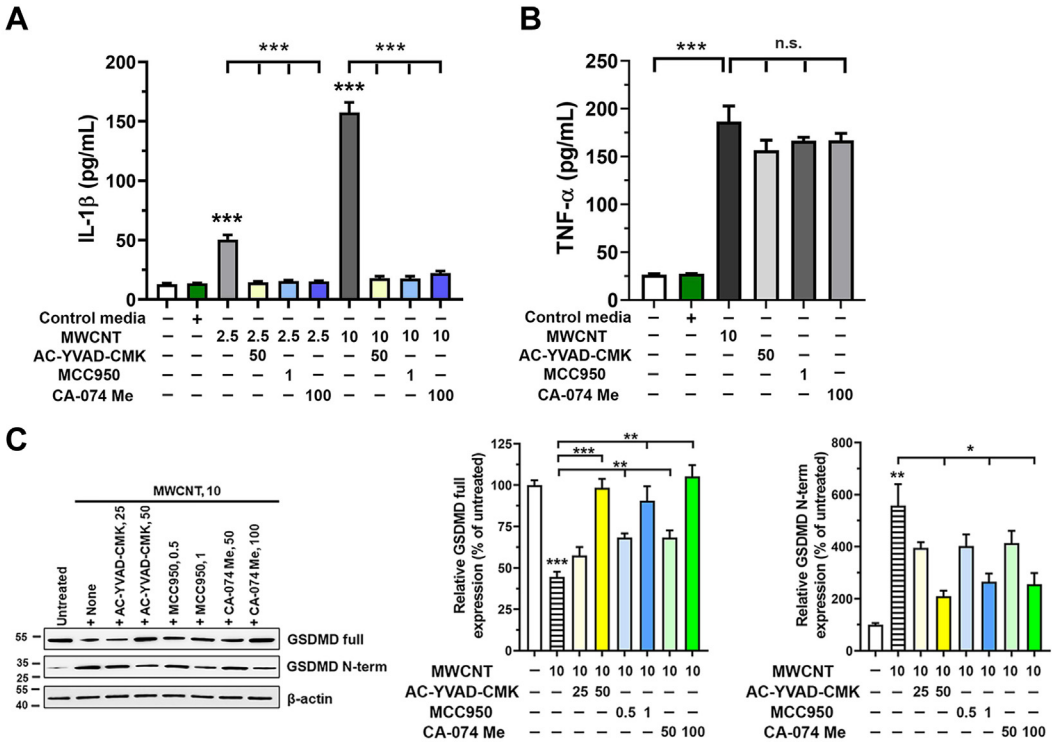

Fig. 5. Inhibition of the NLRP3 inflammasome pathway and pyroptosis induced by MWCNTs in M1 macrophages. (A) and (B) M1 polarized macrophages were incubated with the caspase-1 inhibitor AC-YVAD-CMK at 50 μg/mL, the NLRP3 inflammasome inhibitor MCC-950 at 1 μM, or the cathepsin B inhibitor CA-074 Me at 100 μM for 6 hours before exposing to MWCNTs at 2.5 or 10 μg/mL or CB at 10 μg/mL. IL-1β (A) or TNF-α (B) in cell-free culture supernatants were quantified using ELISA. Data represent mean ± SEM (n = 3). ***, $P <$ .001, significance for comparison to "untreated" control or "MWCNT-treated" group. (C) M1 polarized macrophages were incubated with inhibitors and were exposed treatments as described for (A) and (B) above. GSDMD and GSDMD-N were detected and quantified using immunoblotting and image analysis. Representative images were shown from 3 different experiments. Data represent mean ± SEM *, $P <$ .05, **, $P <$ .01, and ***, $P <$ .001, significance for comparison to compared with "untreated" control or "MWCNT-treated" group; n.s., non-significance at $P =$ .339 for comparison between "AC-YVAD-CMK" and "MWCNT, 10"; $P =$ .199 for comparison between "MCC-950" and "MWCNT, 10," or $P =$ .299 for comparison between "CA-074" and "MWCNT, 10."

partially blocked GSDMD cleavage and GSDMD-N generation. At 50 μg/mL, the inhibitor completely blocked the cleavage of GSDMD cleavage and production of GSDMD-N induced by MWCNTs. The NLRP3 inhibitor MCC-950 at 0.5 or 1 μM, and cathepsin B inhibitor CA-074 Me at 50 or 100 μM, inhibited the generation of GSDMD-N significantly in M1 macrophages.

Taken together, the results from the inhibition experiment support the notion that once phagocytosed by M1 macrophages, MWCNTs trigger lysosomal instability to release cathepsin B into the cytoplasm where a cascade of events was initiated, leading to the NLRP3 inflammasome activation, caspase-1 activation, cleavage of pro-IL-1β and GSDMD, maturation and secretion of IL-1β, and, ultimately, pyroptotic death of the cell.

4. Discussion

Inflammation is commonly observed in the pulmonary response to inhaled nanoparticles in mammalian lungs (Dong and Ma, 2015). The pathogenesis and morphological features of nanoparticle-induced inflammation resemble those of nonmicrobial, respirable particulate-induced pulmonary inflammation, hence, the name sterile inflammation. In these scenarios, deposition of nanoparticles in the airways and the alveolar space triggers the infiltration of neutrophils and the phagocytosis of nanoparticles by alveolar and interstitial macrophages, resulting in innate immune responses and inflammation in the lung. Although inflammation facilitates particle clearance and the debridement of damaged tissues, heightened inflammatory responses cause acute toxicity in the lung. Unresolved inflammation can progress to chronic inflammation leading to the development of fibrosis with granuloma-like lesions, lung and pleural malignancy, and reduction of lung function (Mercer et al, 2013; Kasai et al, 2015, 2016; Suzui et al, 2016; Dong and Ma, 2019). The molecular and cellular underpinnings for the initiation and the temporal evolvement of pulmonary inflammation elicited by nanoparticles are complex and have not been well understood. By examining the effect of exposure to fibrogenic MWCNTs in polarized macrophages in vitro, we uncovered in this study that MWCNTs induce pyroptotic death of macrophages, which serves as a major means of nanotoxicity and sterile inflammation by activating the NLRP3 inflammasomal pathway. Given the critical role and common features and pathways of inflammation in nanotoxicity, our findings provide new insights into the mechanism and facilitate the safety evaluation of the pulmonary health effects of inhaled nanoparticles and nanomaterials.

We have previously observed that macrophages polarize to M1 cells upon exposure to toxic MWCNTs, such as Mitsui-7, which promotes the initiation and amplification of acute inflammatory responses in mouse lungs and in cultured cells (Dong and Ma, 2018a; Lim et al, 2023). At a later stage, macrophages adopt an M2 phenotype and mediate the transition from type 1 to type 2 inflammation, which fosters the resolution of inflammation or its chronic progression and fibrosis if inflammation fails to resolve. In the current study, we found that MWCNTs caused differential cytotoxicity in M1 and M2 cells with M1 macrophages being more sensitive than M2 cells to cell damage by MWCNTs. At the molecular level, MWCNTs caused the activation of the NLRP3 inflammasome and caspase-1 in M1 macrophages. Activated caspase-1

cleaves pro-IL-1β to form IL-1β, a molecular step necessary for the maturation and secretion of the proinflammatory cytokine into the ECM and the circulation.

In agreement with the cytotoxicity of MWCNTS on M1 cells, we found that activation of caspase-1 by MWCNTs induced the proteolytic cleavage of GSDMD in the cell to produce the 31 kDa GSDMD-N, the pore-forming polypeptide responsible for the pyroptotic death of macrophages. Pyroptosis represents a specific type of cell death triggered by proinflammatory signals and observed in inflammatory cells such as macrophages (Cookson and Brennan, 2001; Broz et al, 2020). Pyroptotic cell death is caused via pore formation in the plasma membrane, which disrupts the osmotic gradient across the cell membrane, resulting in the swelling of the cell body and rupture of the cell (Liu et al, 2016; Xia et al, 2021). Thus, pyroptosis is distinguished from other forms of cell death, such as apoptosis, necrosis, and ferroptosis, both mechanistically and morphologically (Yuan and Ofengeim, 2024). Rupture of the cell body releases engulfed pathogens and particulates alongside proinflammatory mediators, including IL-1β and IL-18, which further amplify and propagate inflammation in target tissue and systemically. At the molecular level, pyroptosis is mediated through GSDMD-N. Upon its release from GSDMD cleavage, GSDMD-N binds to the plasma membrane and forms pores through high-order oligomerization. Formation of the pores disrupts the osmotic gradient across the cell membrane, causing the swelling and ultimate rupture of the cell body. MWCNTs induced the cleavage of GSDMD and formation of GSDMD-N in M1 cells to cause pyroptotic cell death, which accounts for the increased cytotoxicity of MWCNTs to M1 macrophages compared with M2 cells.

Caspase-1-mediated cleavage of GSDMD depends on the activation of the NLRP3 inflammasome, a supramolecular oligomeric structure that is formed in response to microbial and sterile signals and mediates the caspase-1-dependent maturation and secretion of IL-1β and IL-18 (Tschopp and Schroder, 2010). The NLRP3 inflammasome serves both as an innate immune effector and as an intracellular pattern recognition receptor that recognizes intracellular pathogen-associated molecular patterns and damage-associated molecular patterns to instigate inflammatory responses to microbial and sterile insults, thereby maintaining cellular homeostasis and function (Schroder and Tschopp, 2010; Ma, 2023). Activation of the NLRP3 inflammasome involves a cascade of molecular events that are signal- and context-dependent and are incompletely understood (Swanson et al, 2019; Ma and Lim, 2024). We found that Mitsui-7 MWCNTs stimulate increased production and secretion of IL-1β in M1, but not M2, macrophages, accompanied by ASC speck formation and activation of caspase-1. Induction of IL-1β is effectively inhibited by inhibitors MCC-950, which inhibits the NLRP3 inflammasome and AC-YVAD-CMK that inhibits caspase-1. Together, these results established that MWCNTs activate the NLRP3 inflammasome and caspase-1 for IL-1β maturation and secretion from M1 macrophages. Furthermore, MWCNT-induced cleavage of GSDMD and generation of GSDMD-N were largely inhibited by the inhibitors, demonstrating a critical role of NLRP3 activation in MWCNT-induced pyroptosis of M1 macrophages.

Lysosomes play unique roles in the cellular response to nanoparticles and other particulate insults (Palomäki et al, 2011; Ma and Lim, 2024). We showed that the Mitsui-7 MWCNTs induced the release and activation of lysosomal cathepsin B. Cathepsin B is known to activate the NLRP3 inflammasome through an as-yet-unclear mechanism, leading to the activation of caspase-1. Indeed, the cathepsin B inhibitor, CA-074, completely inhibited both the production of IL-1β from pro-IL-1β and the cleavage of GSDMD to release GSDMD-N. The findings support the notion that phagocytosis of MWCNTs caused lysosomal damage and cathepsin B release to activate the NLRP3 inflammasome causing IL-1β secretion and pyroptosis of the cell.

A major challenge in the safety evaluation and safe design of engineered nanomaterials and products derives from the fact that the structures and physicochemical properties of nanomaterials are complex and vary considerably, which makes it difficult to compare their health effects directly. By comparing the rod-like Mitsui-7 MWCNTs and a carbonous material control, that is, the Printex 90 CB, we found that in contrast to the MWCNTs that induced a large increase in caspase-1-dependent production of IL-1β, CB did not increase the production of IL-1β and GSDMD-N, which correlated with a lack of cathepsin B activity. These results suggest that CB has substantially reduced damaging effect on macrophage lysosomes and, as a result, reduced activation of the NLRP3 inflammasome, caspase-1 cleavage, IL-1β production, as well as GSDMD-N formation and pyroptotic death of the cell. MWCNTs are composed of multilayers of concentric and cylindrical structures made of graphene sheets, whereas CB is an amorphous, carbon-based, aggregate material. The lack of a defined and ordered 3-dimensional structure like those of MWCNTs in CB may account for its reduced toxicity to lysosomes despite the similar carbon chemistry in MWCNTs and CB (Dong and Ma, 2016). Substantial differences in the shape, size, surface area, surface reactivity, and rigidity between the MWCNTs and CB are noted and may also account for the differences in the activity and toxicity of CB and MWCNTs. A comparison of the transmission electron microscopic images of Mitsui-7 MWCNTs and the CB reviewed that although the diameters of the nanotubes and the CB particles are similar to each other in the range of 50 nm, the nanotubes are rod-like in shape with high rigidity and reach ~4.46 μm in length; however, the CB particles are approximately equal in width and length, thus are substantially smaller than the MWCNTs in size, which would make it easier for macrophages to engulf and handle compared with Mitsui-7 MWCNTs (Ma-Hock et al, 2013; Lim et al, 2023). Further studies on the interplay between nanoparticles and lysosomes in NLRP3 activation and cell death are warranted. Obtaining such knowledge would provide insights into the adverse effect of exposure to nanoparticles in relation to their structures to aid in the safety evaluation and safety-by-design of nanomaterials and products for industrial and commercial applications.

Activation of the NLRP3 inflammasome has been associated with a wide range of disease conditions ranging from autoinflammatory disease and microbial infection to metabolic disease, aging, neurodegeneration, cancer, and common inflammatory and autoimmune diseases such as asthma, rheumatoid arthritis, and Gout, besides many exogenous toxicant-induced disease and toxicity. In this connection, the NLRP3 pathway provides a score of druggable targets for the treatment of human disease. Indeed, pharmacological inhibition of NLRP3 has demonstrated promising efficacy in treating diseases where activation of NLRP3 inflammasomes is implicated in animal models (Ma, 2023; Vande Walle and Lamkanfi, 2024). Our findings on NLRP3- and caspase 1-dependent activation of pyroptosis as a major means of cell death and amplification of inflammation support the notion that activation of GSDMD and its downstream events to induce pyroptotic cell death serve as potential, druggable targets for treating diseases, such as autoinflammation and autoimmune disorders, chronic inflammatory disease, neurodegenerative disease, and cancer, that are difficult to treat at the present time.

Abbreviations

ASC, apoptosis-associated speck-like protein containing a C-terminal caspase recruitment domain; CB, carbon black; CNT, carbon nanotube; FBS, fetal bovine serum; GSDMD, gasdermin D; LPS, lipopolysaccharides; MWCNT, multiwalled carbon nanotube;

NLRP3, NOD-like receptor family, pyrin domain containing 3; TNF, tumor necrosis factor.

Disclaimer

The findings and conclusions in this report are those of the authors and do not necessarily represent the official position of the National Institute for Occupational Safety and Health, Centers for Disease Control and Prevention.

Financial support

This work was supported by the Nanotechnology Research Center program under Grant 9390LGV (Q.M.) at the National Institute for Occupational Safety and Health, Centers for Disease Control and Prevention, USA.

Conflict of interest

The authors declare no conflicts of interest.

Data availability

The authors declare that all the data supporting the findings of this study are contained within the paper.

Authorship contributions

Participated in research design: Lim, Ma.
Conducted experiments: Lim.
Performed data analysis: Lim, Gu.
Wrote or contributed to the writing of the manuscript: Lim, Gu, Ma.

References

Broz P, Pelegrín P, and Shao F (2020) The gasdermins, a protein family executing cell death and inflammation. *Nat Rev Immunol* **20**:143–157.
Chen GY and Nuñez G (2010) Sterile inflammation: sensing and reacting to damage. *Nat Rev Immunol* **10**:826–837.
Cookson BT and Brennan MA (2001) Pro-inflammatory programmed cell death. *Trends Microbiol* **9**:113–114.
Donaldson K, Aitken R, Tran L, Stone V, Duffin R, Forrest G, and Alexander A (2006) Carbon nanotubes: a review of their properties in relation to pulmonary toxicology and workplace safety. *Toxicol Sci* **92**:5–22.
Dong J and Ma Q (2015) Advances in mechanisms and signaling pathways of carbon nanotube toxicity. *Nanotoxicology* **9**:658–676.
Dong J and Ma Q (2016) In vivo activation of a T helper 2-driven innate immune response in lung fibrosis induced by multi-walled carbon nanotubes. *Arch Toxicol* **90**:2231–2248.
Dong J and Ma Q (2018a) Macrophage polarization and activation at the interface of multi-walled carbon nanotube-induced pulmonary inflammation and fibrosis. *Nanotoxicology* **12**:153–168.
Dong J and Ma Q (2018b) Type 2 Immune mechanisms in carbon nanotube-induced lung fibrosis. *Front Immunol* **9**:1120.
Dong J and Ma Q (2019) Integration of inflammation, fibrosis, and cancer induced by carbon nanotubes. *Nanotoxicology* **13**:1244–1274.
Dong J, Porter DW, Batteli LA, Wolfarth MG, Richardson DL, and Ma Q (2015) Pathologic and molecular profiling of rapid-onset fibrosis and inflammation induced by multi-walled carbon nanotubes. *Arch Toxicol* **89**:621–633.
He X, Young SH, Schwegler-Berry D, Chisholm WP, Fernback JE, and Ma Q (2011) Multiwalled carbon nanotubes induce a fibrogenic response by stimulating reactive oxygen species production, activating NF-κB signaling, and promoting fibroblast-to-myofibroblast transformation. *Chem Res Toxicol* **24**:2237–2248.
Hindman B and Ma Q (2019) Carbon nanotubes and crystalline silica stimulate robust ROS production, inflammasome activation, and IL-1beta secretion in macrophages to induce myofibroblast transformation. *Arch Toxicol* **93**:887–907.
Jessop F and Holian A (2015) Extracellular HMGB1 regulates multi-walled carbon nanotube-induced inflammation in vivo. *Nanotoxicology* **9**:365–372.
Kasai T, Umeda Y, Ohnishi M, Kondo H, Takeuchi T, Aiso S, Nishizawa T, Matsumoto M, and Fukushima S (2015) Thirteen-week study of toxicity of fiber-like multi-walled carbon nanotubes with whole-body inhalation exposure in rats. *Nanotoxicology* **9**:413–422.
Kasai T, Umeda Y, Ohnishi M, Mine T, Kondo H, Takeuchi T, Matsumoto M, and Fukushima S (2016) Lung carcinogenicity of inhaled multi-walled carbon nanotube in rats. *Part Fibre Toxicol* **13**:53.
Keshavan S, Gupta G, Martin S, and Fadeel B (2021) Multi-walled carbon nanotubes trigger lysosome-dependent cell death (pyroptosis) in macrophages but not in neutrophils. *Nanotoxicology* **15**:1125–1150.
Lim CS, Porter DW, Orandle MS, Green BJ, Barnes MA, Croston TL, Wolfarth MG, Battelli LA, Andrew ME, Beezhold DH, et al (2020) Resolution of pulmonary inflammation induced by carbon nanotubes and fullerenes in mice: role of macrophage polarization. *Front Immunol* **11**:1186.
Lim CS, Veltri B, Kashon M, Porter DW, and Ma Q (2023) Multi-walled carbon nanotubes induce arachidonate 5-lipoxygenase expression and enhance the polarization and function of M1 macrophages in vitro. *Nanotoxicology* **17**:249–269.
Liu X, Zhang Z, Ruan J, Pan Y, Magupalli VG, Wu H, and Lieberman J (2016) Inflammasome-activated gasdermin D causes pyroptosis by forming membrane pores. *Nature* **535**:153–158.
Ma Q (2020) Polarization of immune cells in the pathologic response to inhaled particulates. *Front Immunol* **11**:1060.
Ma Q (2023) Pharmacological inhibition of the NLRP3 inflammasome: structure, molecular activation, and inhibitor-NLRP3 interaction. *Pharmacol Rev* **75**:487–520.
Ma Q and Lim CS (2024) Molecular activation of NLRP3 inflammasome by particles and crystals: a continuing challenge of immunology and toxicology. *Annu Rev Pharmacol Toxicol* **64**:417–433.
Ma-Hock L, Strauss V, Treumann S, Küttler K, Wohlleben W, Hofmann T, Gröters S, Wiench K, van Ravenzwaay B, and Landsiedel R (2013) Comparative inhalation toxicity of multi-wall carbon nanotubes, graphene, graphite nanoplatelets and low surface carbon black. *Part Fibre Toxicol* **10**:23.
Mercer RR, Scabilloni JF, Hubbs AF, Battelli LA, McKinney W, Friend S, Wolfarth MG, Andrew M, Castranova V, and Porter DW (2013) Distribution and fibrotic response following inhalation exposure to multi-walled carbon nanotubes. *Part Fibre Toxicol* **10**:33.
Murray PJ, Allen JE, Biswas SK, Fisher EA, Gilroy DW, Goerdt S, Gordon S, Hamilton JA, Ivashkiv LB, Lawrence T, et al (2014) Macrophage activation and polarization: nomenclature and experimental guidelines. *Immunity* **41**:14–20.
Palomäki J, Välimäki E, Sund J, Vippola M, Clausen PA, Jensen KA, Savolainen K, Matikainen S, and Alenius H (2011) Long, needle-like carbon nanotubes and asbestos activate the NLRP3 inflammasome through a similar mechanism. *ACS Nano* **5**:6861–6870.
Porter DW, Hubbs AF, Mercer RR, Wu N, Wolfarth MG, Sriram K, Leonard S, Battelli L, Schwegler-Berry D, Friend S, et al (2010) Mouse pulmonary dose- and time course-responses induced by exposure to multi-walled carbon nanotubes. *Toxicology* **269**:136–147.
Porter DW, Orandle M, Zheng P, Wu N, Hamilton RF Jr, Holian A, Chen BT, Andrew M, Wolfarth MG, Battelli L, et al (2020) Mouse pulmonary dose- and time course-responses induced by exposure to nitrogen-doped multi-walled carbon nanotubes. *Inhal Toxicol* **32**:24–38.
Schroder K and Tschopp J (2010) The inflammasomes. *Cell* **140**:821–832.
Shi J, Zhao Y, Wang K, Shi X, Wang Y, Huang H, Zhuang Y, Cai T, Wang F, and Shao F (2015) Cleavage of GSDMD by inflammatory caspases determines pyroptotic cell death. *Nature* **526**:660–665.
Suzui M, Futakuchi M, Fukamachi K, Numano T, Abdelgied M, Takahashi S, Ohnishi M, Omori T, Tsuruoka S, Hirose A, et al (2016) Multiwalled carbon nanotubes intratracheally instilled into the rat lung induce development of pleural malignant mesothelioma and lung tumors. *Cancer Sci* **107**:924–935.
Swanson KV, Deng M, and Ting JP (2019) The NLRP3 inflammasome: molecular activation and regulation to therapeutics. *Nat Rev Immunol* **19**:477–489.
Tschopp J and Schroder K (2010) NLRP3 inflammasome activation: the convergence of multiple signalling pathways on ROS production? *Nat Rev Immunol* **10**:210–215.
Vande Walle L and Lamkanfi M (2024) Drugging the NLRP3 inflammasome: from signalling mechanisms to therapeutic targets. *Nat Rev Drug Discov* **23**:43–66.
Wynn TA and Barron L (2010) Macrophages: master regulators of inflammation and fibrosis. *Semin Liver Dis* **30**:245–257.
Wynn TA, Chawla A, and Pollard JW (2013) Macrophage biology in development, homeostasis and disease. *Nature* **496**:445–455.
Wynn TA and Vannella KM (2016) Macrophages in tissue repair, regeneration, and fibrosis. *Immunity* **44**:450–462.
Xia S, Zhang Z, Magupalli VG, Pablo JL, Dong Y, Vora SM, Wang L, Fu TM, Jacobson MP, Greka A, et al (2021) Gasdermin D pore structure reveals preferential release of mature interleukin-1. *Nature* **593**:607–611.
Yuan J and Ofengeim D (2024) A guide to cell death pathways. *Nat Rev Mol Cell Biol* **25**:379–395.